

## Structure-Based Design of a Potent, Selective, and Irreversible Inhibitor of the Catalytic Domain of the erbB Receptor Subfamily of Protein Tyrosine Kinases

Juswinder Singh,<sup>\*,†</sup> Ellen M. Dobrusin,<sup>‡</sup> David W. Fry,<sup>‡</sup> Taraneh Haske,<sup>‡</sup> Adrian Whitty,<sup>†</sup> and Dennis J. McNamara<sup>‡</sup>

Parke-Davis Pharmaceutical Research, Division of Warner-Lambert Company, 2800 Plymouth Road, Ann Arbor, Michigan 48106-1047, and Biogen Inc., 12 Cambridge Center, Massachusetts 02142

Received May 28, 1996<sup>®</sup>

We report the use of structure-based drug design to create a selective erbB-1 (a.k.a. epidermal growth factor receptor) and erbB-2 (a.k.a. neu/her2 growth factor receptor) tyrosine kinase inhibitor. Using the X-ray crystal structure of the ternary complex of the cAMP-dependent Ser/Thr kinase<sup>1</sup> together with a sequence alignment of the catalytic domains of a representative set of Ser/Thr and Tyr protein kinases, we have examined the nucleotide binding site for potential positions to attach an irreversible inhibitor. This information, combined with homology modeling of the erbB-1 and erbB-2 tyrosine kinase catalytic domains, has led to the identification of Cys797 of erbB1 and Cys805 of erbB2, which are structurally equivalent to Glu127 in the cAMP dependant Ser/Thr kinase as potential target residues. The X-ray structure of the cAMP Ser/Thr kinase shows Glu127 to be involved in a hydrogen-bonding interaction with the 2'-OH of the ribose portion of ATP. Using molecular modeling, it was predicted that the Cys side chains in erbB-1 and erbB-2 performed an analogous role, and it was postulated that the replacement of the 2'-OH of adenosine with a thiol might allow for a covalent bond to form. Since only erbB-1 and erbB-2 have a Cys at this position, the inhibitor should be selective. This model was subsequently tested experimentally by chemical synthesis of 2'-thioadenosine and assayed against the full length erbB-1 receptor and the catalytic domains of erbB-2, insulin receptor,  $\beta$ -PDGF receptor, and the FGF receptor. Our results show that thioadenosine covalently inactivates erbB-1 with a second-order rate constant of  $k_{\max}/K_S = 2000 \pm 500 \text{ M}^{-1} \text{ s}^{-1}$ . Inactivation is fully reversed by 1 mM dithiothreitol, suggesting that inactivation involves the modification of a cysteine residue at the active site, presumably Cys797. The rate of inactivation saturates with increasing thioadenosine concentrations, suggesting that inactivation occurs through initial formation of a noncovalent complex with  $K_D = 1.0 \pm 0.3 \mu\text{M}$ , followed by the slow formation of a disulfide bond with a rate constant of  $k_{\max} = (2.3 \pm 0.2) \times 10^{-3} \text{ s}^{-1}$ . This approach may have application in the design of selective irreversible inhibitors against other members of the kinase family.

### Introduction

The elucidation of the components of the signal transduction pathways are providing new intervention points in the treatment of cancer. One exciting target is the erbB receptor family which includes erbB-1 receptor (a.k.a. EGF receptor) and erbB-2 receptor (a.k.a. neu and her-2 receptor), both of which are transmembrane proteins which, on ligand binding, activate cytoplasmic catalytic domains involved in tyrosine phosphorylation. The overexpression of the erbB-1 receptor has been shown to produce neoplastic phenotype in cells<sup>2-4</sup> and transgenic mice<sup>5</sup> while overexpression of erbB-2 occurs at high frequency in human breast and ovarian carcinomas.<sup>6,7</sup>

While the search for antagonists targeted at the extracellular ligand binding portions of growth factor receptors has proved difficult, there exist compounds known to block their cytoplasmic tyrosine kinase activity. Of these inhibitors, those which compete for binding with peptide substrate have in general been low in potency, moderate in selectivity, and difficult to optimize. However, several examples now exist of ATP competitive inhibitors which are selective against Ser/Thr and Tyr kinases, as well as between Tyr kinases,

which are potent, and inhibit cellular transformation.<sup>8,9</sup> One example are the 4-substituted quinazolines, which are picomolar inhibitors of the EGF receptor and have been shown to block oncogenic transformation.<sup>10</sup> These and other inhibitor classes have been reviewed elsewhere.<sup>11,12</sup> However, structural insight into the means by which these inhibitors act is not available.

An alternative, rational approach would be to use information about the mode of ligand binding to these enzymes to design inhibitors. Over the last decade a wealth of sequence information on the protein kinase family has been generated.<sup>13,14</sup> There currently exists over 200 different protein kinase sequences in the Swissprot database, with the possible number of such proteins being estimated to be a thousand.<sup>15</sup> Over the last several years, crystallographic methods have been used to provide atomic detail to the structure and function of several members of the Ser/Thr<sup>16-20</sup> and Tyr kinase family.<sup>21</sup> The studies have provided insight into both peptide and ATP molecular recognition by these enzymes, as well as providing clues as to their mechanism of activation and inactivation.<sup>22</sup>

Here we report the use of structure-based drug design to design a selective irreversible nucleoside inhibitor to the erbB receptor subfamily of protein tyrosine kinases. The work described here is an extension of a comparative analysis<sup>23</sup> of sequence conservation between the Ser/Thr and Tyr kinases in the context of the structure

\* To whom correspondence should be addressed.

<sup>†</sup> Biogen Inc.

<sup>‡</sup> Parke-Davis Pharmaceutical Research.

<sup>®</sup> Abstract published in *Advance ACS Abstracts*, February 15, 1997.

of the cAMP dependent Ser/Thr kinase.<sup>1,16,17</sup> Here we specifically address the conservation of Cys residues in the nucleotide binding site of the kinase family and how this could be exploited to design specific inhibitors. Also we describe the experimental testing of our model-building studies. As far as we are aware, these results are the first example of structure-based drug design on the erbB receptor family and provide a conceptual framework for the design of inhibitors against other members of the kinase family.

## Results and Discussion

### Prediction of erbB Nucleotide Binding Site.

Figure 1 shows a sequence alignment of the catalytic domains of several members of the protein kinase family.<sup>13</sup> In order to assess the feasibility of designing irreversible nucleoside inhibitors against members of the kinase family we examined the conservation of sequence (and thereby structure) in their nucleotide binding sites. Using the ternary complex of cAPK, which had been determined by X-ray crystallography,<sup>1</sup> we defined the nucleotide binding site as those protein residues within 4.5 Å of ATP. Using the sequence alignment we inferred the nucleotide binding site of the other kinases by extrapolation of those defined in cAPK (Figure 1). It consists of 21 residues, of which 6 of these residue positions in the alignment are invariant and an additional 6 positions are almost invariant, with most of these sequences involving a single residue substitution at this position. The majority of the remaining nine positions involve exchanges between more than two related amino acids. The strong conservation of sequence suggested that the mode of binding of ATP was likely to be the same throughout the family and thus provided a structural framework for the design of nucleoside inhibitors. Although the rational design of specific noncovalent inhibitors would be predicted to be difficult since the ATP binding sites are similar, the distribution of Cys residues, with their thiol moieties capable of forming disulfide bonds with sulfur-containing inhibitors, provided a means for the design of specific irreversible inhibitors. Interestingly, none of the Ser/Thr kinases were predicted to have a Cys in the nucleotide binding site, while five of the seven Tyr kinases have a Cys. In addition, the distribution of Cys residues among the Tyr kinase suggested that formation of a covalent attachment to different Cys residues could result in the selective inhibition of different Tyr kinases. Our hypothesis was that a selective inhibitor against both erbB-1 and erbB-2 could be formed by linking to Cys797 of erbB-1 or Cys805 of erbB-2 (structurally equivalent to Glu127 of cAPK).

### Model Building of erbB-1 and erbB-2 Catalytic

**Domains.** The viability of developing a selective inhibitor of erbB-1 and erbB-2 was assessed through constructing molecular models of ATP binding to these proteins based upon the ternary complex of cAPK. Figure 2 shows the contacts formed between adenosine and the nucleotide binding sites of cAPK and erbB-2. (This is identical to that seen in erbB-1.) The known ternary structure of cAPK shows that position 127 is a Glu residue in which the carboxylate is involved in a hydrogen-bonding interaction with the 2'-hydroxyl of the ribose moiety of ATP (Figure 2a). The conservation of a hydrogen-bonding residue at this position in the other kinases suggests a similar role is played in other members of the family. This is supported by the struc-

ture of Cys127 and the adenosine portion of ATP in our model-built structure of the erbB-1 and erbB-2. The geometry of the Cys residue is ideal for a hydrogen-bonding interaction between its sulfhydryl and the ribose hydroxyl (Figure 2b). This suggested that replacement of the 2'-OH with a sulfhydryl to form a thioadenosine derivative might allow for a covalent disulfide bond to form. Rather than synthesizing the 2'-thio analog of ATP, we focused on the more chemically accessible nucleoside derivative, 2'-thioadenosine, assuming it would bind similarly. This assumption was supported by experimental data from cAPK which shows most of the binding energy of ATP complexing to the enzyme comes from the adenosine portion and not the triphosphate portion ( $K_d$  ATP 10  $\mu$ M; ADP 10  $\mu$ M; adenosine 35  $\mu$ M).<sup>24</sup> To explore the structural implications of the covalent linkage we built a model of the covalently attached thioadenosine/Cys127 protein complex to both erbB-1 and erbB-2. The minimized structures suggested little structural perturbation to the nucleotide binding site and to the conformation of adenosine relative to the noncovalent complexes.

**Inhibition of erbB Catalytic Activity by Thioadenosine.** The above hypothesis was tested experimentally by chemically synthesizing 2'-thioadenosine and measuring its inhibitory potency against a panel of protein tyrosine kinases. Adenosine was also tested to specifically assess the importance of a sulfhydryl at the 2'-position. Figure 3 shows the time-dependent loss of kinase activity of full-length erbB-1 when incubated with 0.2–6.25  $\mu$ M thioadenosine for various times before being assayed, as described in the Experimental Section. The pseudo-first-order rate constant for inactivation increases with increasing concentrations of thioadenosine, as shown in Figure 4, displaying a hyperbolic dependence that saturates at a maximum rate constant for inactivation of  $k_{max} \approx 0.15 \text{ min}^{-1}$ . Data measured at the highest concentrations of thioadenosine tested, up to 25  $\mu$ M, show increased scatter (Figure 4, inset); however, including all of the data in the fit has only a small effect on the  $k_{max}$  and  $K_S$  values obtained from the data. From the data in Figure 4 we calculate that thioadenosine inactivates erbB-1 with a second-order rate constant of  $k_{max}/K_S = 2000 \pm 500 \text{ M}^{-1} \text{ s}^{-1}$ , with a maximum rate of  $k_{max} = (2.3 \pm 0.2) \times 10^{-3} \text{ s}^{-1}$  and a half-saturating thioadenosine concentration of  $K_S = 1.0 \pm 0.3 \mu\text{M}$ . After incubation of erbB-1 with a 5  $\mu$ M thioadenosine for a period that was shown to result in ~70% inhibition of the kinase activity, the activity of the enzyme could be fully restored by treatment with 1 mM dithiothreitol, suggesting that inactivation by thioadenosine involves modification of a free cysteine residue at the active site of erbB-1, presumably Cys797. This result and the kinetic data thus suggest a two-step inactivation mechanism, involving the initial formation of a noncovalent complex with  $K_D \approx 1 \mu\text{M}$ , followed by the slow formation of a disulfide bond between the thioadenosine and Cys797. The rate constant for the slow irreversible step,  $k_{max} \approx 2.3 \times 10^{-3} \text{ s}^{-1}$ , corresponds to a half-time of  $5 \pm 0.5 \text{ min}$  for the formation of the disulfide bond within the initially-formed encounter complex.

Minus a thiol group at the 2'-position, adenosine itself was a much less potent inhibitor of erbB-1, having an  $IC_{50}$  of 195  $\mu$ M under comparable conditions (data not shown). ErbB-2 also was substantially more sensitive

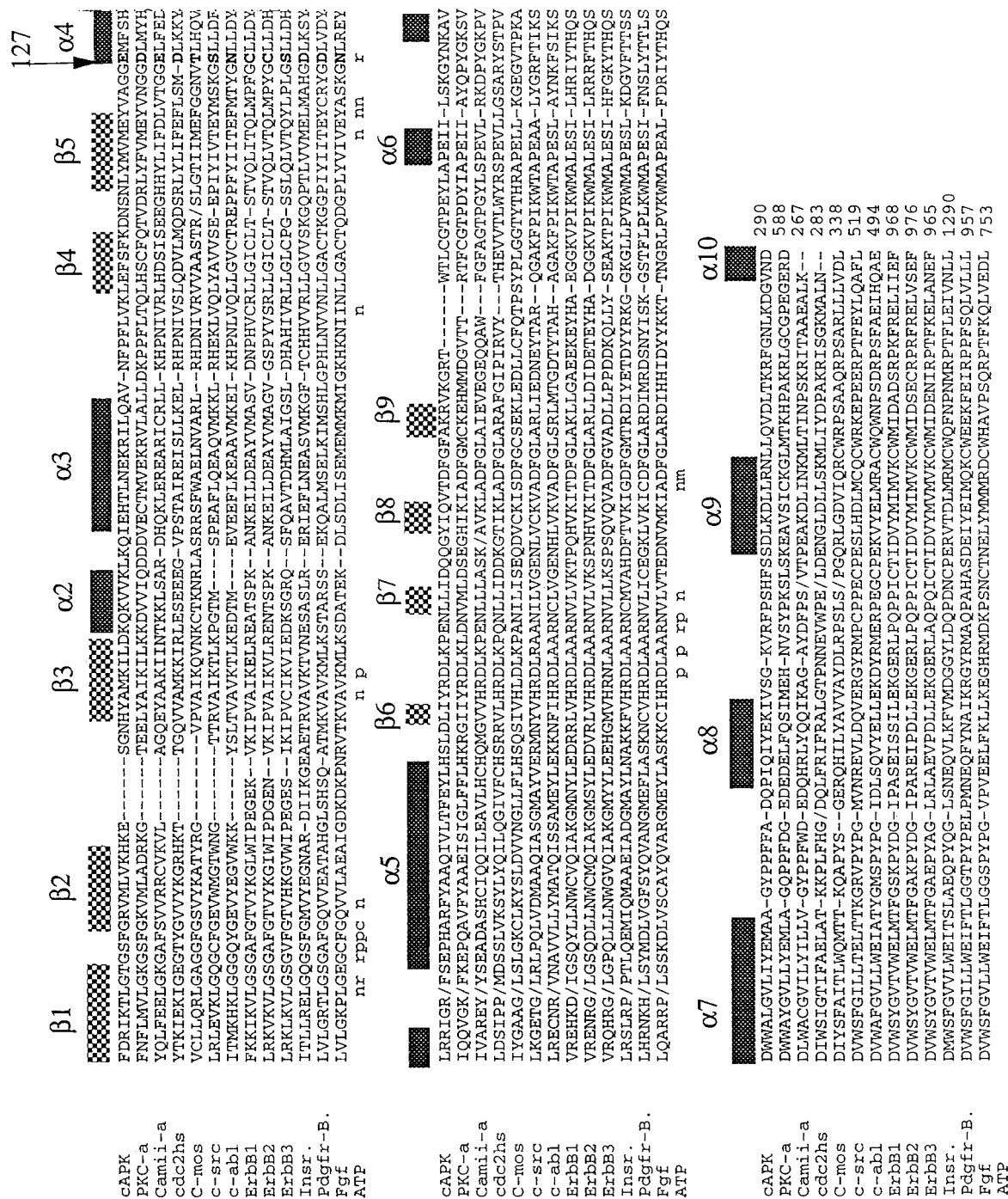


**Figure 1.** Sequence alignment of a representative set of the protein kinase family. The sequence alignment is based upon that described by Hanks et al.<sup>13</sup> The secondary structure was taken from the crystal structure of the ternary complex of cAMP dependent Ser/Thr kinase (cAPK).<sup>1</sup> The nucleotide binding site of the cAPK is defined in the ATP row. The letters denote the type of interaction the residue forms with ATP; an n indicates a contact between the protein and the purine portion of adenosine, r is ribose, p is phosphate, c is a nonspecific contact, and m is metal. The arrow denotes position 127 (cAPK numbering system) which was determined to be suitable for the design of an irreversible and specific kinase inhibitor against erbB-1 and erbB-2.

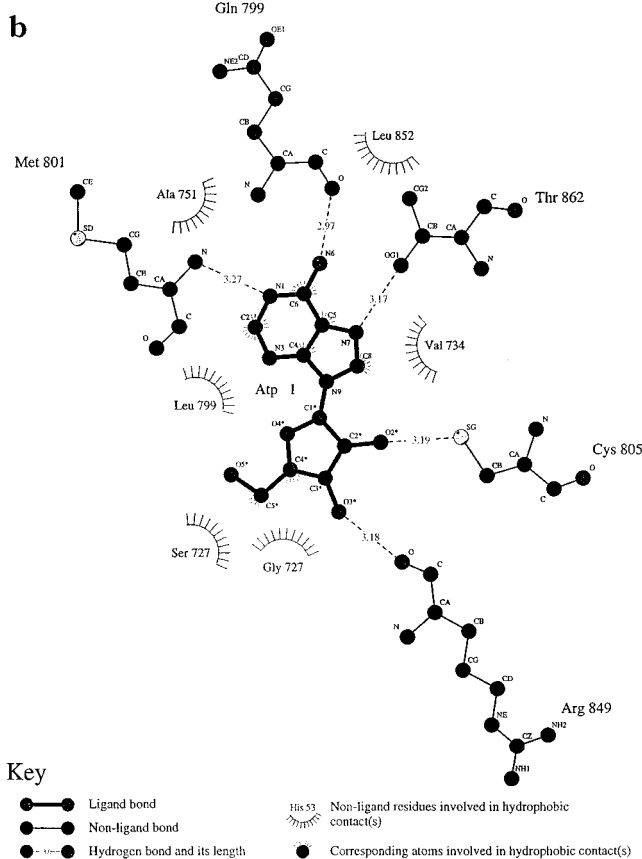
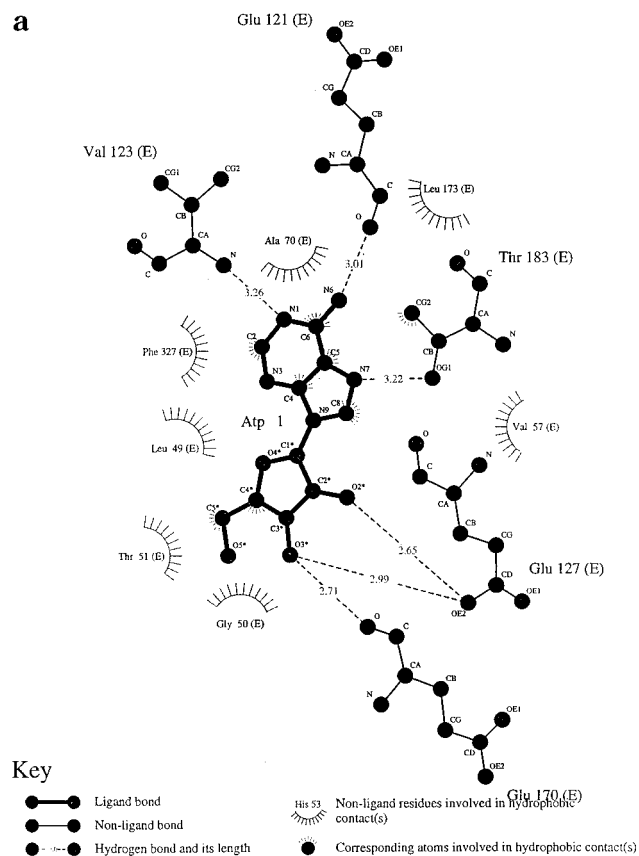


**Figure 2.** Schematic plots of the contacts between adenosine and the nucleotide binding sites of (a) cAPK and (b) erbB-2 generated using LIGPLOT.<sup>37</sup> The bonds of the ligand are shown by a thick line, whereas the enzyme is shown by thin lines. Dashed lines represent hydrogen bonds with distances given in angstroms. The spiked arms represent hydrophobic interactions (defined by non-bonded carbon-carbon contacts of <math><3.9\text{ \AA}</math>).

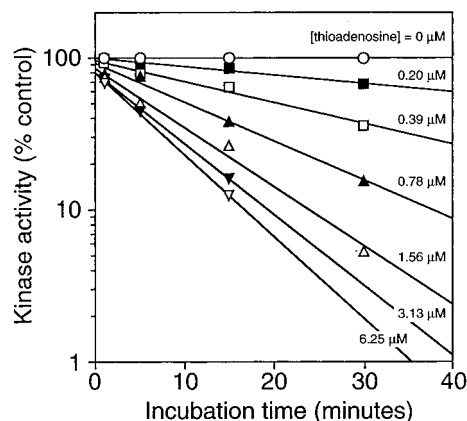


**Figure 3.** Semilogarithmic plots showing the time-dependent inactivation of full-length erbB-1 by various concentrations of thioadenosine. The enzyme was incubated with 0.1–25  $\mu\text{M}$  thioadenosine in kinase assay buffer containing all components except ATP. Reactions were initiated after incubation periods of 1, 5, 15, or 30 min by adding ATP to the reaction mixtures, as described in the Experimental Section. Kinase activity is expressed as percent of control. For clarity, curves are shown in the figure for a subset of thioadenosine concentrations from 0.2–6.25  $\mu\text{M}$ , as indicated on the plot. Small deviations in the percent activity at zero incubation time are due to a small amount of inactivation that occurs during the kinase assay itself. Experiments were performed in duplicate.

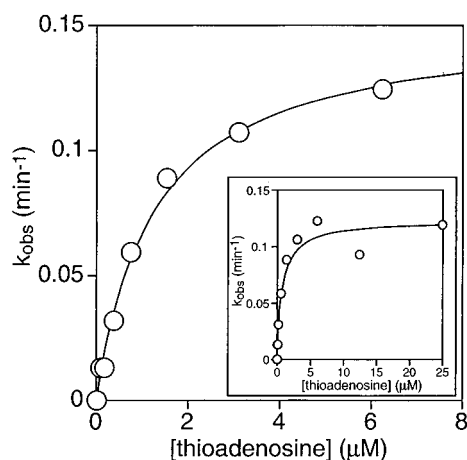


**Figure 4.** Observed rate constants for inactivation of erbB-1 by 0.1–6.25  $\mu\text{M}$  thioadenosine, measured as described in the legend to Figure 3. The solid line is a hyperbolic fit to the data, as described in the text. Inset plot: data for all thioadenosine concentrations tested (0.1–25  $\mu\text{M}$ ), showing that including even the less accurate data measured at higher thioadenosine concentrations does not significantly alter the result (details are given in the text). Experiments were performed in duplicate.

to inhibition by 2'-thioadenosine (50% inhibition achieved at 45  $\mu\text{M}$  thioadenosine upon 10 min incubation) than by adenosine ( $\text{IC}_{50} \approx 1.6\text{ mM}$ ). Neither adenosine nor thioadenosine exhibited activity against FGF, PDGF or insulin receptor tyrosine kinases at 50  $\mu\text{M}$  (data not shown).

Interpretation of the rate saturation in Figure 4 in terms of the formation of a noncovalent complex between thioadenosine and erbB-1 with  $K_S \approx 1\text{ }\mu\text{M}$  suggests the 2'-thiol group, in addition to allowing the formation of a disulfide bond with the enzyme, may also confer some additional noncovalent binding affinity over that seen with adenosine. However, the inhibition by adenosine was measured in the presence of ATP, and so the  $\text{IC}_{50}$  that was determined for adenosine may be larger than the actual  $K_S$  for the binding of this

compound to the active site because of competition by the ATP.

## Conclusion

Due to the important role of protein kinases in controlling cell division and differentiation, the identification of their selective inhibitors is an active area of drug discovery research.<sup>10–12</sup> This may be facilitated through the availability of structural information on these proteins which should make them amenable for structure-based drug design. Our work has described the use of molecular modeling based upon ATP binding to the cAMP Ser/Thr kinase to design a nucleoside inhibitor specific to erbB-1 and erbB-2 through the subtle modification of the 2'-hydroxyl of adenosine to a thiol. Our model for ATP binding is supported by recent structural information on ATP binding to other members of the protein kinase family. The structures of cyclin-dependent protein kinase 2 (CDK2) is now known with ATP bound.<sup>25</sup> For cAPK and CDK2, the binding mode of the adenosine portion of ATP is similar, while the triphosphate portion is different and supports our hypothesis of adenosine binding to erbB-1 and erbB-2 will be similar to that seen in the above kinases. For example, in CDK2 the contact seen in cAPK between Glu127 and the ribose 2'-OH is functionally replaced by an Asp. The X-ray structure of the insulin receptor is the only tyrosine kinase structure known.<sup>21</sup> Our alignment predicts that as for CDK2 an Asp functionally replaces Glu127 in the insulin receptor; however this has not been experimentally verified since the current structure exists in the inactive state without ATP bound.

We have created a potent and selective tyrosine kinase inhibitor. Inactivation of erbB-1 was shown to be time-dependent and reversible by DTT and to display kinetic features consistent with a two-step inactivation mechanism. Each of these features, plus the much greater sensitivity of erbB-1 and erbB-2 to inhibition by thioadenosine compared to adenosine, and the fact that thioadenosine inhibits only erbB-1 and erbB-2 out of the panel of kinases tested, supports our predicted mode of inhibition by formation of a disulfide bond with Cys797 in the active site of erbB-1.

The X-ray structure determination of how these inhibitors bind would be useful to confirm our model. The structure of CDK2 bound to two inhibitors, olomoucine and isopentenyladenine, has been determined, both of which are competitive inhibitors of ATP and both of which bind in a different orientation to that seen for ATP.<sup>25</sup> However, our nucleoside analog represents a subtle derivative of adenosine and combined with the predicted covalent nature of the interaction suggests more confidence in our model.

There exist advantages in the design of irreversible inhibitors for controlling cellular transformation. Such an irreversible inhibitor might result in prolonged suppression of the tyrosine kinase activity of the EGF receptor with a single dose compared to the more frequent administration required for a reversible inhibitor. We are currently performing cellular studies to assess the *in vivo* activity of these compounds. There also exists the possibility for optimizing these inhibitors. One suggestion will be to take advantage of the polar interactions formed by the phosphate portion of the nucleotide. As mentioned earlier the  $K_d$  for adenosine binding to cAPK is 35  $\mu\text{M}$  while that of ADP and ATP

is 10  $\mu\text{M}$ .<sup>34</sup> Therefore we predict 3–5-fold improvement in binding by the modification of thioadenosine to thioadenosine di- or triphosphate.

## Experimental Section

**Sequence and Structure Analysis of the Protein Kinase Family.** A multiple sequence alignment of protein kinases was generated based upon a previous alignment<sup>13</sup> but was slightly modified to include structural information from the cAMP dependent Ser/Thr kinase.<sup>1</sup> The sequences were obtained from the March 1992 version of the Catalytic Domain Database (distributed by S. K. Hanks and A. M. Quinn, The Salk Institute for Biological Studies). This sequences chosen for alignment were based according to a subfamily classification,<sup>13</sup> with only one member of each being represented (Figure 1). The five Ser/Thr kinases used were cAPK (mouse cyclic-AMP dependent Ser/Thr Kinase), PKC- $\alpha$  (rat protein kinase C alpha), Camii-A (rat calcium-calmodulin dependent kinase II alpha subunit), Cdc2hs (cell division control protein 2), C-Mos (human cellular homolog of v-mos). The eight Tyr kinases were C-Src (human cellular homolog of v-src), C-Abl (human cellular homolog of v-abl), erbB-1 (human epidermal growth factor receptor), erbB-2 (human oncogene product, a.k.a. Neu and HER2), erbB-3 (gene product related to epidermal growth factor receptor), Insr (human insulin receptor), Pdgf-B (human platelet derived growth factor receptor, B-type), and the Fgf (human fibroblast growth factor receptor). The X-ray coordinates of cAPK complexed with a peptide inhibitor and ATP<sup>1,16,17</sup> was obtained from the Brookhaven Databank (Brookhaven code pdb1atp.ent).<sup>26</sup>

The sequence of the murine cAPK for which the 3D structure has been determined was aligned with respect to the other kinase sequences. In order to explore the influence of sequence variation on the known 3D structure of the protein kinase, we considered only those residues in the protein kinase catalytic domains which could be aligned to the murine cAPK. The analysis described here includes residues 43–290 (using the numbering scheme of cAPK). This was chosen since the definition of the kinase domain in the sequence file varies, and according to the definition of Hanks et al. (1988)<sup>13</sup> this includes the 11 conserved subdomains. Those residues of the cAPK structure within 4.5 Å of ATP were defined as the nucleotide binding site.

**Model Building of the Catalytic Domains of ErbB-1 and ErbB-2.** Using homology modeling,<sup>27</sup> we have constructed a 3D model of the catalytic domain of erbB-1 and erbB-2 using the X-ray structure of the ternary complex of cAPK as the template. From the sequence alignment of the protein kinase family described above we have substituted those side chains from cAPK with those seen in erbB-1 and erbB-2. The conformation of the side chains were built using the side chain optimization program Maxsprout.<sup>28</sup> Those side chains common between cAPK and erbB-1 and cAPK and erbB-2 were held fixed during the model building procedure. This was based upon studies which have shown that, in general, topologically equivalent side chains in homologous structures adopt the same torsion angles.<sup>29,30</sup> The structure of ATP was taken from the cAPK and fitted into an equivalent position in the two models. These were then subjected to 100 cycles of energy minimization using the Powell optimization procedure and the Amber forcefield as implemented in the Sybyl modelling package<sup>31</sup> using the Kollman united atom charges.<sup>32</sup>

**Purification of Epidermal Growth Factor Receptor Tyrosine Kinase.** Full-length human erbB-1 receptor tyrosine kinase was isolated from A431 human epidermoid carcinoma cells by the method described in Gill and Weber.<sup>33</sup> Briefly, cells were grown in roller bottles in dMEM/F12 media (Gibco) containing 10% fetal calf serum. Approximately  $10^9$  cells were lysed in two volumes of buffer containing 20 mM Hepes, pH 7.4, 5 mM EGTA, 1% Triton X-100, 10% glycerol, 0.1 mM sodium *o*-vanadate, 5 mM sodium fluoride, 4 mM pyrophosphate, 4 mM benzamide, 1 mM DTT, 80  $\mu\text{g}/\text{mL}$  aprotinin, 40  $\mu\text{g}/\text{mL}$  leupeptin, and 1 mM PMSF. After centrifugation at 25000g for 10 min, the supernatant was equilibrated for 2 h at 4 °C with 10 mL of sepharose conjugated

with anti-EGF receptor antibody.<sup>33</sup> Contaminating proteins were washed from the resin with 1 M NaCl followed by 1 mM urea. The enzyme was eluted with 0.1 mg/mL EGF. The receptor appeared to be homogeneous as assessed by Coomassie blue stained polyacrylamide gels.

**Recombinant Kinases.** The intracellular domains of p185<sup>erbB-2</sup>,  $\beta$ -PDGF receptor, FGF-1 receptor, and insulin receptor were obtained as described previously.<sup>34</sup>

**Tyrosine Kinase Assays.** Enzyme reactions for the full-length erbB-1 receptor tyrosine kinase were performed in a total volume of 0.1 mL containing 25 mM Hepes, pH 7.4, 5 mM MgCl<sub>2</sub>, 2 mM MnCl<sub>2</sub>, 5–10 ng of enzyme, and 10  $\mu$ M ATP containing 1  $\mu$ Ci of [<sup>32</sup>P]ATP, varying concentrations of nucleoside and 100  $\mu$ g of a random polymer of tyrosine and glutamic acid (Sigma).

All components except the ATP were added to the wells. In certain experiments, the enzyme was preincubated with inhibitor for varying times as described in the figure legends. The reaction was initiated by the addition of [<sup>32</sup>P]ATP and incubated at 25 °C for 10 min. The reaction was terminated with 10% trichloroacetic acid (TCA) and the precipitate washed twice with ice-cold TCA. Radioactivity was determined by scintillation counting.

Assays using intracellular kinase domains were performed in a total volume of 100  $\mu$ L containing 50 mM HEPES buffer (pH 7.4), 10 mM MnCl<sub>2</sub>, 10  $\mu$ M [<sup>32</sup>P]ATP, 100  $\mu$ g of a random polymer of tyrosine and glutamic acid (Sigma), and 100–500 ng of enzyme. The reaction was initiated by the addition of [<sup>32</sup>P]ATP and incubated at 25 °C for 10 min. The reaction was terminated with 10% TCA, and the precipitate washed twice with ice-cold TCA. Radioactivity was determined by scintillation counting.

**Chemical Synthesis.** Adenosine (PD047028) was purchased from Sigma. 2'-Thioadenosine (PD157432) was synthesized as described<sup>35</sup> except that the 6-amino group of adenine was not protected.<sup>36</sup>

**Acknowledgment.** We would like to thank Kumud Kaur-Singh for critical evaluation of the manuscript. We would like to also acknowledge the useful suggestions of one of the reviewers. The authors may be contacted by e-mail at juswinder\_singh@biogen.com.

## References

- Zheng, J.; Knighton, D. R.; Ten Eyck, L. F.; Karlsson, R.; Xuong, N.; Taylor, S. S.; Sowadski, J. M. Crystal structure of the catalytic subunit of the cAMP Ser/Thr-dependent protein kinase complexed with MgATP and peptide inhibitor. *Biochemistry* **1993**, *32*, 2154–2161.
- Riedel, H.; Massoglia, J.; Schlessinger, J.; Ullrich, A. Ligand activation of overexpressed epidermal growth factor receptors transforms NIH 3T3 mouse fibroblasts. *Proc. Natl. Acad. Sci. U.S.A.* **1988**, *85*, 1477.
- Velu, T. J.; Beguinot, L.; Vass, W. C.; Willingham, M. C.; Merlino, G. T.; Pastan, I.; Lowy, D. R. Epidermal growth factor dependent transformation by a human EGF receptor proto-oncogene. *Science* **1987**, *238*, 1408.
- Stern, D. F.; Hare, D. L.; Cecchini, M. A.; Weinberg, R. A. Construction of a novel oncogene based upon synthetic sequences encoding epidermal growth factor receptor. *Science* **1987**, *235*, 321.
- Sandgren, E. P.; Luetette, N. C.; Palmiter, R. D.; Brinster, R. L.; Lee, D. C. Overexpression of TGF  $\alpha$  in transgenic mice: induction of epithelial hyperplasia, pancreatic metaplasia and carcinoma of the breast. *Cell* **1990**, *61*, 1121.
- Slamon, D. J.; Godolphin, W.; Jones, L. A.; Holt, J. A.; Wong, S. G.; Keith, D. E.; Levin, W. J.; Stuart, S. G.; Udove, J.; Ullrich, A.; et al. Studies of the HER-2/neu proto-oncogene in human breast and ovarian cancer. *Science* **1989**, *244*, 707.
- Bacus, S. S.; Stancovski, I.; Huberman, E.; Chin, D.; Hurwitz, E.; Mills, G. B.; Ullrich, A.; Sela, M.; Yarden, Y. Tumour-inhibitory monoclonal antibodies to the HER-2/Neu receptor induce differentiation of human breast cancer cells. *Cancer Res.* **1992**, *52*, 2580.
- Fry, D. W.; Kraker, A. J.; McMichael, A.; Ambrosio, L. A.; Nelson, J. M.; Leopold, W. R.; Connors, R. W.; Bridges, A. A specific inhibitor of the epidermal growth factor receptor tyrosine kinase. *Science* **1994**, *265*, 1093–1095.
- Ward, W. H. J.; Cook, P. N.; Slater, A. M.; Davies, D. H.; Holdgate, G. A.; Green, L. R. Epidermal growth factor receptor tyrosine kinase. Investigation of catalytic mechanism, structure based searching and discovery of a potent inhibitor. *Biochem. Pharmacol.* **1994**, *48*, 659–666.
- Fry, D. W. Protein tyrosine kinases as therapeutic targets: Cancer Chemotherapy and Recent advances in development of new inhibitors. *Expert Opin. Invest. Drugs* **1994**, *3*, 577–595.
- Levitzi, A.; Gazit, A. Tyrosine kinase inhibition: An approach to drug development. *Science* **1995**, *267*, 1782–1788.
- Bridges, A. Current status of tyrosine kinase inhibitors: Do the diarylamine inhibitors of the EGFR represent a new beginning? *Expert Opin. Ther. Pat.* **1995**, *5*, 1245–1257.
- Hanks, S. K.; Quinn, A. M.; Hunter, T. The protein kinase family: Conserved features and deduced phylogeny of the catalytic domains. *Science* **1988**, *241*, 42–51.
- Hanks, S. K.; Quinn, A. M. Protein kinase catalytic domain sequence database: identification of conserved features of primary structure and classification of family members. *Methods Enzymol.* **1991**, *200*, 38–62.
- Hunter, T. A thousand and one protein kinases. *Cell* **1987**, *50*, 823–829.
- Knighton, D. R.; Zheng, J.; Ten Eyck, L. F.; Ashford, V. A.; Xuong, N. H.; Taylor, S. S.; Sowadski, J. M. Crystal structure of the catalytic subunit of cyclic adenosine monophosphate-dependent protein kinase. *Science* **1991**, *253*, 407–413.
- Knighton, D. R.; Zheng, J.; Ten Eyck, L. F.; Xuong, N. H.; Taylor, S. S.; Sowadski, J. M. Structure of a peptide inhibitor bound to the catalytic subunit of cyclic adenosine monophosphate-dependent protein kinase. *Science* **1991**, *253*, 414–420.
- De Bondt, H. L.; Rosenblatt, J.; Jancarik, J.; Jones, H. D.; Morgan, D. O.; Kim, S. H. Crystal structure of cyclin-dependent kinase 2. *Nature* **1993**, *363*, 595–602.
- Hu, S. H.; Parker, M. W.; Lei, J. Y.; Wilce, M. C.; Benian, G. M.; Kemp, B. E. Insights into autoregulation from the crystal structure of twitchin kinase. *Nature* **1994**, *369*, 581–584.
- Zhang, F.; Strand, A.; Robbins, D.; Cobb, M. H.; Goldsmith, E. J. Atomic structure of the MAP kinase ERK2 at 2.3 Å resolution. *Nature* **1994**, *367*, 704–711.
- Hubbard, S. R.; Wei, L.; Ellis, L.; Hendrickson, W. A. Crystal structure of the tyrosine kinase domain of the human insulin receptor. *Nature* **1994**, *372*, 746–754.
- Bossemeyer, D. Protein Kinases structure and function. *FEBS Lett.* **1995**, *369*, 57–61.
- Singh, J. Comparison of conservation within and between the Ser/Thr and Tyr protein kinase family: proposed model for the catalytic domain of the epidermal growth factor receptor. *Protein Eng.* **1994**, *7*, 849–858.
- Bhatnager, D.; Roskoski, R., Jr.; Rosendahl, M. S.; Leonard, N. J. Adenosine cyclic 3',5'-monophosphate dependent protein kinase: A new fluorescence displacement titration technique for characterizing the nucleotide binding site on the catalytic subunit. *Biochemistry* **1983**, *22*, 6310–6317.
- Schulze-Gahmen, U.; Brandsen, J.; Jones, H. D.; Morgan, D. O.; Meijer, L.; Vesely, J.; Kim, S. H. Multiple modes of ligand recognition: crystal structures of cyclin-dependent protein kinase 2 in complex with ATP and two inhibitors, olomoucine and isopentenyladenine. *Proteins: Struct. Funct. Genet.* **1995**, *22*, 378–391.
- Bernstein, F. C.; Koetzle, T. F.; Williams, G. J. D.; Meyer, E. F.; Brice, M. D.; Rodgers, J. R.; Kennard, O.; Schimanochi, T.; Tasumi, M. The protein databank; a computer-based archival for macromolecular structures. *J. Mol. Biol.* **1977**, *112*, 535–542.
- Blundell, T. L.; Sibanda, B. L.; Sternberg, M. J. E.; Thornton, J. M. Knowledge-based prediction of protein structures and the design of novel molecules. *Nature* **1987**, *326*, 347–352.
- Holm, L.; Sander, C. Fast and simple Monte Carlo algorithm for side chain optimization in proteins: application to model building by homology. *Proteins: Struct. Funct. Genet.* **1992**, *14*, 213–223.
- Lesk, A. M.; Chothia, C. H. The response of protein structures to amino-acid sequence changes. *Phil. Trans. R. Soc. London, Ser. A* **1986**, *317*, 345–356.
- Summers, N. L.; Carlson, W. D.; Karplus, M. Analysis of side-chain orientations in homologous proteins. *J. Mol. Biol.* **1987**, *196*, 175–198.
- Sybyl6.0. Tripos Associates Inc., St. Louis, MO.
- Weiner, S. J.; Kollman, D. A.; Case, D. A.; Singh, U. C.; Ghio, C.; Alagona, G.; Profeta, S.; Weiner, P. K. *J. Am. Chem. Soc.* **1984**, *106*, 765–784.
- Gill, G. N.; Weber, W. Purification of functionally active epidermal growth factor receptor protein using a competitive antagonist monoclonal antibody and competitive elution with epidermal growth factor. *Methods Enzymol.* **1987**, *146*, 82–88.
- Fry, D. W.; Kraker, A. J.; Connors, R. C.; Elliott, W. L.; Nelson, J. H.; Showalter, H. D.; Leopold, W. R. Strategies for the discovery of novel tyrosine kinase inhibitors with anticancer activity. *Anti-Cancer Drug Des.* **1994**, *9*, 331–351.
- Marriot, J. H.; Mottahedeh, M.; Reese, C. B. Synthesis of 2'-thioadenosine. *Carbohydr. Res.* **1991**, *216*, 257–269.
- Robins, M. J.; Hawrelak, S. D.; Hernandez, A. E.; Wnuk, S. F. Efficient general synthesis of purine (amino, azido and triflate)-sugar nucleosides. *Nucleosides Nucleotides* **1992**, *11*, 821–834.
- Wallace, A. C.; Laskowski, R. A.; Thornton, J. M. *Protein Eng.* **1995**, *8*, 127–134.